EUROFUSION WPPMI-PR(16) 16572

S.K. Kim et al.

# Dependence of Pedestal Properties on Plasma Parameters in European DEMO

Preprint of Paper to be submitted for publication in
Nuclear Fusion

This work has been carried out within the framework of the EUROfusion Consortium and has received funding from the Euratom research and training programme 2014-2018 under grant agreement No 633053. The views and opinions expressed herein do not necessarily reflect those of the European Commission.

# Dependence of Pedestal Properties on Plasma Parameters in European DEMO

**S.K. Kim[1], Y-s. Na[1], S. Saarelma[2], and O. Kwon[3*]**

[1]Department of Nuclear Engineering, Seoul National University, Gwanak 08826, Seoul, Korea
[2]Euratom/CCFE Fusion Association, Culham Science Centre, OX14 3DB, Abingdon, UK
[3]Department of Physics, Daegu University, Gyeongsan 38453, Gyeongbuk, Korea

[*]e-mail : ojkwon@daegu.ac.kr

**Abstract**

We have numerically investigated the dependence of pedestal properties such as the pedestal height and the pedestal width on various global parameters using the EURO-DEMO as reference equilibrium. We have used EPED, a predictive model of the edge pedestal. Among global parameters we have chosen to vary, the triangularity, $\delta$, the elongation, $\kappa$, and the poloidal beta, $\beta_p$, have larger effect on the pedestal properties. Improvement of pedestal properties can be achieved for more shaped plasma boundary. However, the increase in the pedestal height and the width with $\delta$ saturates around $\delta \sim 0.6$. Also, the pedestal width saturates and the pedestal temperature starts to decrease for $\kappa > 1.9$. Improvement of the pedestal properties due to $\delta$ is larger at higher poloidal beta. The pedestal width slightly increases with the electron density at the pedestal top and the effective charge number.

## 1. Introduction

The next step in the development of fusion energy after the ITER project currently under construction in France, is the so-called DEMO reactor that will demonstrate the production of electricity from fusion power. The general guidelines in the design of DEMO are outlined in previous studies [1, 2]. A more specific design for European DEMO (EURO-DEMO1) is presented in Ref. 3. One of the key requirements for any DEMO design is reasonably high energy multiplication factor Q, i.e. the fusion energy produced divided by the energy used heating the plasma. The main effect on Q comes from plasma confinement; The better the confinement is, the easier it is to reach high value of Q. The confinement in H-mode can be divided into two components, the confinement in the core region, which is dominated by turbulent transport that restricts the temperature gradient $\nabla T/T$ below a critical value due to so-called stiff transport and the confinement of the pedestal near the edge where the density and temperature gradients can be significantly steeper than in the core due to suppression of turbulent transport. Instead of turbulence, the H-mode pedestals are ultimately limited by the MHD instabilities such as peeling-ballooning modes (PBM) [4]. In the EPED model [5], the PB stability criterion is combined with a criterion for the kinetic ballooning modes (KBM) to give a prediction for the pedestal temperature.

In this paper, we investigate the parameter dependencies of the EURO-DEMO1 design [3] in the EPED1 framework, which first creates a series of equilibria with the pedestal height and width ($\Delta_{ped}$) being tied by the condition, $\Delta_{ped} = 0.076\sqrt{\beta_{p,ped}}$, where $\beta_{p,ped}$ is the poloidal $\beta$ at the top of the pedestal. Then the pedestal prediction is the equilibrium corresponding to the crossing of the stability boundary for PBMs. The equilibria are solved including the self-consistent bootstrap using the model by Sauter [6] implemented in HELENA code [7]. The stability of the equilibria is solved using the MISHKA-1 code [8].

The design parameters are the following; Major radius ($R_0$): 9.1m, minor radius (a): 2.9m, plasma current ($I_p$) 19.6 MA, toroidal magnetic field at geometrical axis ($B_t$): 5.7 T, elongation at the plasma boundary ($\kappa$): 1.78, triangularity at the plasma boundary ($\delta$): 0.45, global poloidal $\beta$ ($\beta_p$): 1.1, electron density at the top of the pedestal ($n_{e,ped}$): $6.8 \times 10^{19}/m^3$, effective charge ($Z_{eff}$): 2.58 and the charge of the main impurity, Xenon ($Z_{imp}$): 54. We vary these parameters around the nominal values and perform EPED predictions. To gain insight on the physics behind the effects on EPED predictions, we then investigate more in detail how the changes in EPED predictions are related to the changes in equilibrium and PBM stability.

## 2. Results

### 2.1 Effect of plasma boundary shaping parameters

The geometric characteristic of plasma boundary is usually defined by triangularity and elongation. Since $\delta$ and $\kappa$ can change various plasma parameters such as the safety factor, current density and pressure gradient not only in the core but also at pedestal region, they can strongly affect MHD instabilities including PBM in edge region. As a result, pedestal structure may strongly depend on the plasma shape. To find the effect of the plasma shaping on the pedestal properties, we calculated the height and width of the edge pedestal by changing $\delta$ and $\kappa$ separately from the reference equilibrium. The results are shown in Fig. 1. From this figure, it can be seen that $\Delta_{ped}$ and $T_{ped}$ ($T_{ped}$ is the temperature at the top of the pedestal) vary considerably with $\kappa$ and $\delta$, for low to moderate values. Both $\Delta_{ped}$ and $T_{ped}$ increase as both shape parameters increase. These results agree well with various experiment findings [9-13]. Fig. 1(a) shows that $\Delta_{ped}$ increases by 70%, while $T_{ped}$ increases threefold, as $\delta$ changes from 0 to 0.5. When $\kappa$ varies from 1.4 to 1.8, $\Delta_{ped}$ and $T_{ped}$ improve by 60% as shown in Fig. 1(b). The reason for improved pedestal structure turned out to be the increased stabilization of PBM, as manifested in Fig. 2 which shows the stability boundary of PBM on $j_\phi - \alpha$ space, where $\alpha = -(2\mu_0 q^2/\epsilon B_T^2)(\partial P/\partial \rho)$ [14] is normalized pressure gradient, and $j_\phi$ is edge current density. Both $j_\phi$ and $\alpha$ values are their maximum near the center of the edge pedestal region. Here, $q$ is safety factor, $\rho$ is normalized radius, $\epsilon$ is inverse aspect ratio, $P$ is plasma pressure, and $B_T$ is toroidal magnetic field at magnetic axis. As $\delta$ and $\kappa$ increase, stability region widens and it allows plasma equilibrium to move diagonally to the region of larger $\alpha$

and $j_\phi$. This will lead to improved pedestal structure, due to the fact that $\alpha$ and $\Delta_{ped}$ are correlated under KBM condition [5,15] in the EPED model, where the following Eq. (1) is satisfied,

$$\alpha \propto P_{ped}/\Delta_{ped} \propto \beta_{p,ped}/\Delta_{ped} \propto \Delta_{ped} \propto T_{ped}^{1/2}. \quad (1)$$

Here $P_{ped}$ is plasma pressure at pedestal top. Therefore, larger $\alpha$ will make $\Delta_{ped}$ wider and $T_{ped}$ higher. Also, $T_{ped}$ increases faster than $\Delta_{ped}$ because $T_{ped} \propto \Delta_{ped}^2$. As a consequence, both $\Delta_{ped}$ and $T_{ped}$ can increase as the stability boundary widens when $\delta$ and/or $\kappa$ increase to moderate values. This is consistent with previous studies of shaping effect on PBM [16-19].

Large improvement in pedestal properties with plasma boundary shaping observed for low to moderate $\kappa$ and $\delta$ values cannot be sustained as shaping becomes stronger. In Fig. 1(a), it can be seen that $\Delta_{ped}$ and $T_{ped}$ saturates at $\delta > 0.6$. The saturation of pedestal structure with $\delta$ is related to the behavior of trapped fraction, $f_t$. At pedestal region, the toroidal current is dominated by the bootstrap current, $j_{bs}$, which is proportional to pressure gradient ($\propto \alpha$) and $f_t$ [6]. The trapped fraction does not change much with $\delta$ when $\delta$ is small, so both critical $j_\phi$ and $\alpha$ can increase at the same time in $j_\phi - \alpha$ space if the stability boundary widens. But, for large $\delta$, $f_t$ considerably decreases [20], and $j_{bs}$ cannot grow further even if $\alpha$ increases. Fig. 3(a) shows how reduction in $f_t$ can affect the movement of the critical equilibrium. In Fig. 3(a), the critical equilibrium point moves up diagonally (i.e., both critical $j_\phi$ and critical $\alpha$ increase with $\delta$) nearly following the nose of stability boundary for $\delta \leq 0.6$ because $f_t$ remains almost same. When $\delta > 0.6$, however, $j_{bs}$ decreases since $f_t$ decreases as $\delta$ increases. The critical equilibrium point then moves downward accordingly (i.e., critical $j_\phi$ decreases while critical $\alpha$ does not vary much with $\delta$). Therefore, even though the stability boundary still improves for $\delta > 0.6$, the improvement cannot be fully utilized because $j_\phi$ decreases. As a result, $\Delta_{ped}$ and $T_{ped}$ begins to saturate near $\delta \simeq 0.6$. Comparison of $f_t(\delta)$ with $j_\phi/\alpha$ ($\propto j_{bs}/\nabla P$) as a function of $\delta$ for the critical equilibrium points as shown in Fig. 3(b) shows consistency of this explanation, such that the saturation of $\Delta_{ped}$ and $T_{ped}$ in large $\delta$ is mainly due to $f_t$.

Figure 1(b) also shows that $T_{ped}$ starts to decrease when $\kappa > 1.9$ while $\Delta_{ped}$ steadily increases with $\kappa$. When $\kappa$ changes from 1.9 to 2.3, $\Delta_{ped}$ increases by 10% and $T_{ped}$ decreases by 10%. This phenomenon can be understood from the expression of $T_{ped}$ with $\kappa$. Under the KBM constraint, $T_{ped}$ and $\partial T_{ped}/\partial\kappa$ can be described by Eqs.(2) and (3) when $\kappa$ variation is allowed,

$$T_{ped} \propto \beta_{p,ped} I_p^2/L^2 \propto \Delta_{ped}^2 I_p^2/(\kappa^2+1). \quad (2)$$

$$\partial T_{ped}/\partial\kappa \propto \partial\Delta_{ped}/\partial\kappa - \Delta_{ped}/\kappa. \quad (3)$$

where $I_p$ is plasma current and $L$ is the perimeter of plasma boundary. As shown in Fig. 1(b), $\Delta_{ped}$ increases rapidly with $\kappa$ for $\kappa \leq 1.9$. Therefore, $\partial\Delta_{ped}/\partial\kappa$ is larger than $\Delta_{ped}/\kappa$ in this range. Consequently, $T_{ped}$ increases with $\kappa$ from Eq.(3). On the contrary, $\partial\Delta_{ped}/\partial\kappa$ become smaller than

$\Delta_{ped}/\kappa$ for large κ, because stabilization effect of κ saturates at large shaping. In this range, $\partial T_{ped}/\partial\kappa$ becomes negative when $\kappa > 1.9$ and therefore, $T_{ped}$ decreases as κ increases. This explains the behavior of $T_{ped}$ in Fig. 1(b) as a function of $\kappa$.

### 2.2 Effect of the poloidal beta

Poloidal beta, $\beta_p$, is one of major global parameters in tokamak plasma that indicate the performance of plasma confinement. Since $\beta_p$ has strong dependence on pressure profile and poloidal flux distribution, it affects PBM and pedestal structure. Especially, a previous study found that $\beta_p$ induces Shafranov shift, $\Delta_{sh}$, [21] and that it stabilizes the edge instability via Shafranov stabilization effect [4, 5, 22]. We performed $\beta_p$ scans and results are shown in Fig. 4. In this figure, $\Delta_{ped}$ and $T_{ped}$ are shown to increase as $\beta_p$ increases. This agrees fairly well with the expectation from Shafranov stabilization and also with experimental results [23-27].

Improvement in $\Delta_{ped}$ and $T_{ped}$ with $\beta_p$ is larger at higher δ than at lower δ. As shown in Fig.4, a change in $\Delta_{ped}$ when $\beta_p$ varies from 0.8 to 1.3 is almost negligible (less than 1%) when $\delta = 0.2$, while it becomes larger by more than 15% for $\delta = 0.5$ in the same range of $\beta_p$. This indicates that effect of $\beta_p$ on pedestal structure can be enhanced by strong shaping. A similar trend has been found in experiment [28].

This behavior turned out to be due to higher stabilization effect of $\beta_p$ more dominantly on pure ballooning mode than on the pure peeling mode. Fig.5 shows the edge stability boundaries for two different $\beta_p$ values (0.8 and 1.1) for $\delta = 0.4$. It can be seen that the stability generally improves for larger $\beta_p$, more predominantly in the large α direction. The nose of the stability boundary moves upward only by 10%, while moving to the right in large α direction by 25%, which indicates the stabilization of the ballooning mode. Larger critical α allows the growth of the pedestal structure ($\Delta_{ped}$ and $T_{ped}$), according to Eq. (1). Horizontal distance between noses of different $\beta_p$ values in $j_\phi - \alpha$ space increases as δ increases. The increase in α is only 10% for $\delta = 0$, while it reaches 30% for $\delta = 0.6$, when $\beta_p$ is varied from 0.8 to 1.1. Therefore, difference of pedestal structure in two $\beta_p$ cases is enlarged for higher δ. It can be concluded that the stabilizing effect of δ on edge pedestal is enhanced with $\beta_p$, and vice versa. The mechanism that describes the synergetic stabilization effect of $\beta_p$ and δ on PBM still remains as a question.

### 2.3 Effect of electron density and effective charge number

The effect of electron density at the pedestal top, $n_{e,ped}$, and effective charge number, $Z_{eff}$, on pedestal properties has also been investigated. The effect of $n_{e,ped}$ is shown in Fig. 6(a) for two different values of δ ($\delta = 0.45$ and $\delta = 0.65$). A mode structure of a critical equilibrium with $\delta = 0.45$ shows dominant components due to peeling mode, thus the critical equilibrium being located at left of the nose of the stability diagram in $j_\phi - \alpha$ space. On the other hand, a critical equilibrium with $\delta = 0.65$ has an eigenfuction with dominant components due to ballooning mode.

The critical equilibrium is located at lower right of the nose. In both cases, Fig. 6(a) shows that $\Delta_{ped}$ increases by 10% as $n_{e,ped}$ changes from $3\times10^{19}/m^3$ to $7\times10^{19}/m^3$. However, $T_{e,ped}$ decreases by more than 50% for the same change in $n_{e,ped}$. This can be understood by the KBM constraint in EPED model, where $T_{ped}$ can be expressed as Eq. (4),

$$T_{ped} = P_{ped}/n_{ped} \propto \frac{\Delta_{ped}^2}{n_{e,ped}}\left(2-\frac{Z_{eff}-1}{Z_{imp}}\right)^{-1}. \quad (4)$$

We have used the relation,

$$n_{ped} = n_{e,ped}\left(2-\frac{Z_{eff}-1}{Z_{imp}}\right), \quad (5)$$

which is satisfied for a single species of impurity with the impurity charge number $Z_{imp}$. Since variation of $\Delta_{ped}$ is not large, $1/n_{e,ped}$ term dominates in Eq. (4). Therefore, $T_{e,ped}$ decreases even if $\Delta_{ped}$ slightly increases when $n_{e,ped}$ increases.

The results of $Z_{eff}$ scan are shown in Fig. 6(b), where $\Delta_{ped}$ increases monotonically by 5% as $Z_{eff}$ is varied from 1.5 to 4.5. From Eq. (4), $T_{ped}$ is expected to increase if $\Delta_{ped}$ increases as $Z_{eff}$ increases for fixed $n_{e,ped}$ and $Z_{imp}$. As expected, Fig. 6(b) shows that $T_{ped}$ also increases monotonically with $Z_{eff}$. We assumed a flat $Z_{eff}$ profile in calculation.

The electron density and the effective charge number are found to affect the edge stability through the electron-ion collisionality, $\nu_{ei}$. The collisionality changes resistivity and bootstrap current [29]. Therefore, the edge plasma current distribution will be changed and this has influence on the PBM stability [30, 31]. The dependence of the effective collisionality on $n_{e,ped}$, $Z_{eff}$, and $Z_{imp}$ can be written as Eq. (6),

$$\nu_{eff} \equiv n_{e,ped}^{\frac{5}{2}} Z_{eff} P_{ped}^{-\frac{3}{2}}\left(2-\frac{Z_{eff}-1}{Z_{imp}}\right)^{\frac{3}{2}} \propto Z_{eff} n_{e,ped} T_{ped}^{-\frac{3}{2}} \propto \nu_{ei}. \quad (6)$$

After we expressed the variations of $n_{e,ped}$ and $Z_{eff}$ in terms of that of $\nu_{eff}$, which is normalized to the reference equilibrium value, we have re-plotted previous results of Fig. 6 in Fig. 7. Here, $\nu_{eff}$ varies because either $n_{e,ped}$ or $Z_{eff}$ changes. It can be clearly seen that $\Delta_{ped}$ variations are nearly same in both cases. However, $T_{ped}$ curves show different behavior for obvious reasons, i.e., due to Eqs. (4) and (6). If we have plotted $P_{ped}$ curves instead of $T_{ped}$ curves, they will also show good agreement, of course. Although we have not shown the effect of $Z_{imp}$, we found from its scan that the behavior of the pedestal structure with $Z_{imp}$ can be also understood from the variation of $\nu_{eff}$.

Experimental results of correlation between the pedestal width and the collisionality are not yet clear. They sometimes reach different conclusions even in the same machine. $\Delta_{ped}$ increases with $n_{e,ped}$ in DIII-D and JET [32], as predicted by our calculations. It is also shown to increase with $Z_{eff}$ in JT-60U [33] and with collisionality [34]. In other cases, $\Delta_{ped}$ is shown to decrease with $n_{e,ped}$ in

DIII-D [35,36] and JET [37], or they have not shown any meaningful correlations in JET and DIII-D [38,39].

The critical equilibrium points are plotted with $n_{e,ped}$ variation in Fig. 8 in the $j_\phi - \alpha$ space. The change in stability boundaries is almost negligible unlike when $\delta$, $\kappa$, and $\beta_p$ are varied. The result that $\Delta_{ped}$ increases with $n_{e,ped}$ as shown in Fig. 6(a), seems to contradict our intuition when equilibria are located in the ballooning dominant region due to large shaping of $\delta = 0.65$. It can be seen that the critical $\alpha$ decreases as $n_{e,ped}$ increases in this case, which generally means $\Delta_{ped}$ should also decrease according to Eq. (1). This can be reconciled by considering the fact that a new equilibrium is constructed when $n_{e,ped}$ is varied, and that Eq. (1) cannot be applied for this change. A new equilibrium with increased $n_{e,ped}$ has smaller $\alpha$ and $j_\phi$ for the same $\Delta_{ped}$, such that it enters inside the stability boundary. This then allows $\alpha$ and $\Delta_{ped}$ to increase where Eq. (1) can be applied. Therefore, $\Delta_{ped}$ increases even if the critical $\alpha$ decreases compared to that of the smaller $n_{e,ped}$ equilibrium.

### 3. Conclusions and discussions

With edge predictive model EPED, we determined the temperature at the pedestal top and width of the pedestal when plasma parameters ($\delta$, $\kappa$, $\beta_p$, $n_{e,ped}$ and $Z_{eff}$) are varied. The plasma boundary shaping parameters ($\delta$ and $\kappa$) change plasma equilibrium properties and the PBM stability boundary considerably. These affect the pedestal structure and EPED model predicts that $\Delta_{ped}$ and $T_{ped}$ generally increase with the shaping. This agrees well with experimental findings. However, $\Delta_{ped}$ and $T_{ped}$ saturate or even decrease when $\delta$ and $\kappa$ increase further. The degradation of the edge pedestal improvement for very large $\delta$ cases is due to the drop in the trapped fraction which then makes the bootstrap current decrease. This implies that excessive shaping is less effective as far as the edge pedestal structure is concerned. Large shaping also induces difficulties in plasma control and there exists some limit in plasma operation window. Optimum shaping parameters can be determined by considering both control issues and predictive modeling.

Effect of $\beta_p$ on pedestal structure is also quite large. High $\beta_p$ is favorable because of Shafranov shift stabilization effect dominantly on the ballooning mode, thus changing the stability boundary by increasing the critical pressure gradient. This behavior also agrees well with experimental results. Furthermore, synergetic improvement of edge properties due to $\beta_p$ and shape parameter is found and it is expected that optimization of edge pedestal structure via shaping will be more effective in plasma with higher $\beta_p$.

Increasing $n_{e,ped}$ and $Z_{eff}$ also makes $\Delta_{ped}$ increase. But their influence is quite small compared to that of $\delta$, $\kappa$ and $\beta_p$, because the change in the stability boundary is negligible. Effect of $n_{e,ped}$ and $Z_{eff}$ is shown to be mainly through effective collisionality, thus changing the bootstrap current.

We have performed the parameter scans for EURO-DEMO1 reference case. But our results can be also applied to explanation of edge properties and optimization of edge structure in conventional

tokamaks.

**Acknowledgements**

The first author would like to express the deepest gratitude to the Fusion and Plasma Application Laboratory (FUSMA) Team at Seoul National University for their kind support and fruitful discussions for this paper. This work was supported by the National R&D Program through the National Research Foundation of Korea (NRF), funded by the Ministry of Science, ICT & Future Planning (No. 2014-M1A7A1A03045368) and the R&D Program through the National Fusion Research Institute of Korea (NFRI) funded by the Government funds. The opinions included herein do not reflect those of the National Research Foundation of Korea. This work has been carried out within the framework of the EUROfusion Consortium and has received funding from the Euratom research and training programme 2014-2018 under grant agreement No 633053 and from the RCUK Energy Programme [grant number EP/I501045]. The work is part of the EUROfusion Enabling Research project CfP-WP15-ENR-01/CCFE-03. The views and opinions expressed herein do not necessarily reflect those of the European Commission.

**References**

[1] G.H. Neilson et al. Nucl. Fusion 52 (2012) 047001
[2] H. Zohm et al. Nucl. Fusion 53 (2013) 073019
[3] R. Wenninger, accepted for publication in Nucl. Fusion.
[4] P.B. Snyder et al., Nucl. Fusion 49 (2009) 085035
[5] P.B. Snyder et al., Physics of Plasmas 16 (2009) 056118
[6] O. Satuter et al., Physics of Plasmas 6 (1999) 2834
[7] G.T.A.Huysmans, J.P.Goedbloed, and W.O.K.Kerner, *Proceeding of CP90 Conference on Computational Physics* (World Scientific, Singapore, 1991) p371.
[8] A.B. Mihailovskii et al., Plasma Phys. Rep. 23 (1997) 844.
[9] T.H. Osborne et al., Plasma Phys. Control. Fusion 42 (2000) A174
[10] A.W. Leonard et al., Nucl. Fusion 47 (2007) 552
[11] T.Onjun et al., Phys. Plasma 11 (2004) 3006
[12] A.E. Hubbard et al., Plasma Phys. Control. Fusion 42 (2000) A15
[13] A.Kallenbach et al., Nucl. Fusion 42 (2002) 1184
[14] T. Onjun et al., Phys. Plasma 12 (2005) 082513
[15] D.Dickinson et al., PRL 108 (2012) 135002
[16] P.B. Snyder et al., Physics of Plasmas 9 (2002) 2037
[17] P.B. Snyder et a.,l Plasma Phys. Control. Fusion 46 (2004) A131
[18] T. Ozeki et al., Nucl. Fusion 30 (1990) 1425

[19] R.L. Miller et al., Plasma Phys. Control. Fusion 40 (1998) 753
[20] O. Sauter, A simple formula for the trapped fraction in tokamak including the effect of the triangularity No. EPFL-REPORT-187521 (2013)
[21] L.L.Lao, S.P.Hirshman Phys.Fluids 24, 1431 (1981)
[22] P.B. Snyder et al., Nucl. Fusion 47 (2007) 961
[23] C.F. Maggi et al., Nucl. Fusion 47 (2007) 535
[24] A.W. Leonard, Journal of Physics:Conference Series 123 (2008) 012001
[25] H. Urano et al., Nucl. Fusion 48 (2008) 045008
[26] C.F. Maggi et al., Nucl. Fusion 50 (2010) 025023
[27] I.T. Champman et al., Nucl. Fusion 55 (2015) 013004
[28] Y. Kamada el al., Plasma Phys. Control Fusion 44 (2002) A279
[29] D.M. Thomas el al., Plasma Phys. Control. Fusion 48 (2006) A183
[30] J.W. Connor, Plasma Phys. Control. Fusion 40 (1998) 191
[31] H.R. Wilson et al., Plasma Phys. Control. Fusion 48 (2006) A71[32] D.A. Mossessian., et al 30th EPS Conference (2003,St.Peters burg) ECA Vol.27A P-3.182
[33] H. Urano et al., Nucl. Fusion 55 (2015) 033010
[34] P.A. Schneider., et al Plasma Phys. Control. Fusion 54 (2012) 105009
[35] M.A. Mahdavi et al., Phys. Plasma 10 (2003) 3984
[36] R.J. Groebner et al., Nucl. Fusion 49 (2009) 085037
[37] M. Sugihara et al., Nucl.Fusion 40 (2000) 1743
[38] M.N.A. Beurskens et al., Plasma Phys. Control. Fusion 51 (2009) 124051
[39] M.N.A. Beurskens et al., Phys. Plasma 18 (2011) 056120

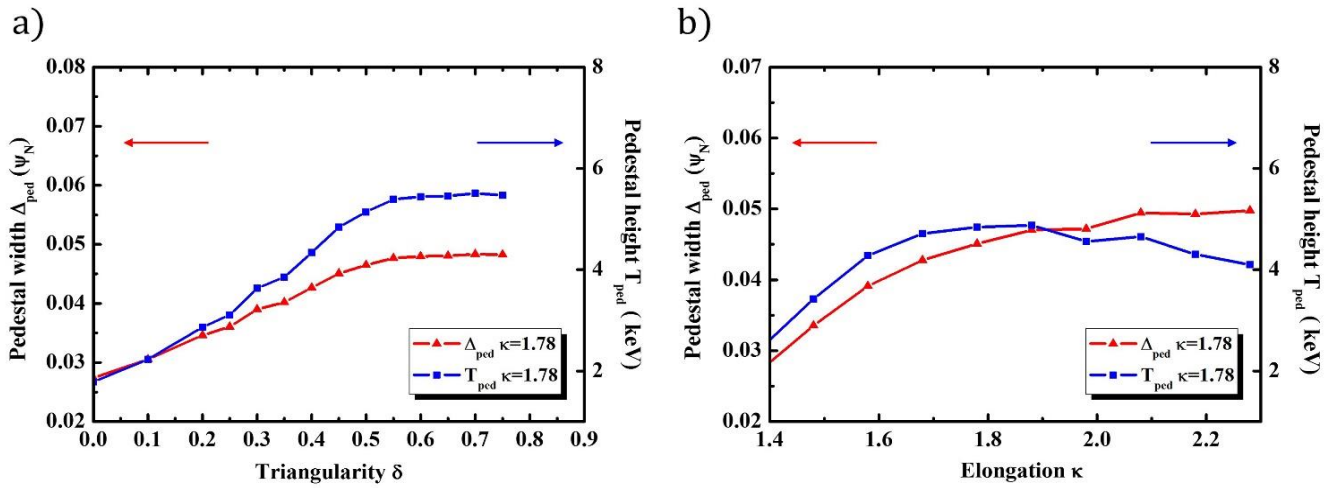


Fig. 1 $\boldsymbol{\Delta_{ped}}$ (in red) and $\boldsymbol{T_{ped}}$ (in blue) as a function of (a) $\boldsymbol{\delta}$ and (b) $\boldsymbol{\kappa}$.

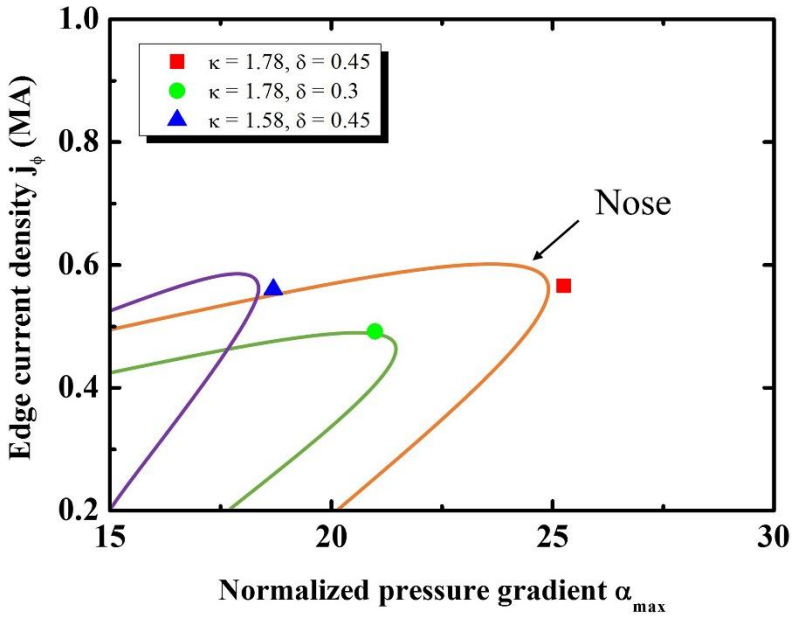


Fig. 2 Figure shows equilibrium points on $\boldsymbol{j_\phi - \alpha}$ space for reference (red), smaller $\boldsymbol{\delta}$ (green) and smaller $\boldsymbol{\kappa}$ (blue) case. The peeling-ballooning stability boundary for each case is also drawn. As either $\boldsymbol{\kappa}$ or $\boldsymbol{\delta}$ increase, the PBM stability boundary expands.

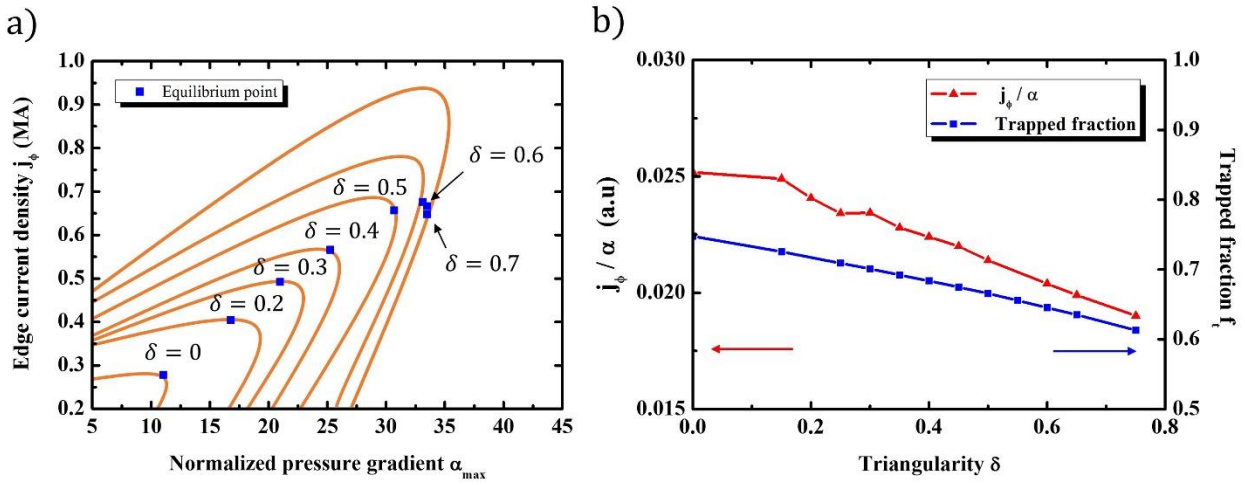


Fig. 3 a) Critical equilibrium points and stability boundaries (orange) for different $\boldsymbol{\delta}$ values. The critical equilibrium moves diagonally for $\boldsymbol{\delta \leq 0.6}$. b) $\boldsymbol{j_\phi/\alpha}$ and $\boldsymbol{f_t}$ as a function of $\boldsymbol{\delta}$. Good agreement can be found between these two curves.

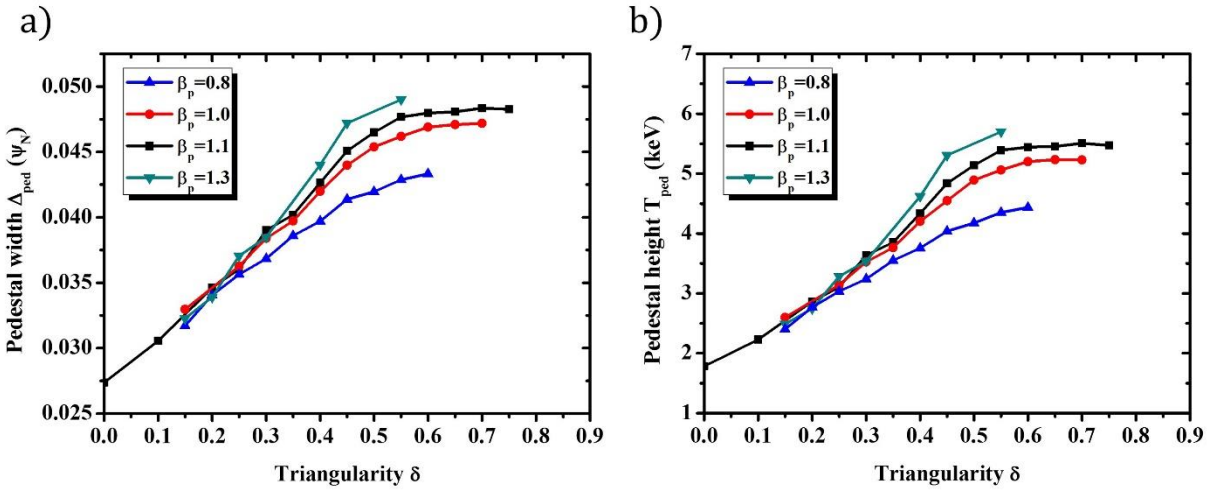


Fig. 4 a) $\boldsymbol{\Delta_{ped}}$ and b) $\boldsymbol{T_{ped}}$ as a function $\boldsymbol{\delta}$ for various $\boldsymbol{\beta_p}$. Both $\boldsymbol{\Delta_{ped}}$ and $\boldsymbol{T_{ped}}$ increase with $\boldsymbol{\beta_p}$ and $\boldsymbol{\delta}$, and saturate for $\boldsymbol{\delta \geq 0.6}$.

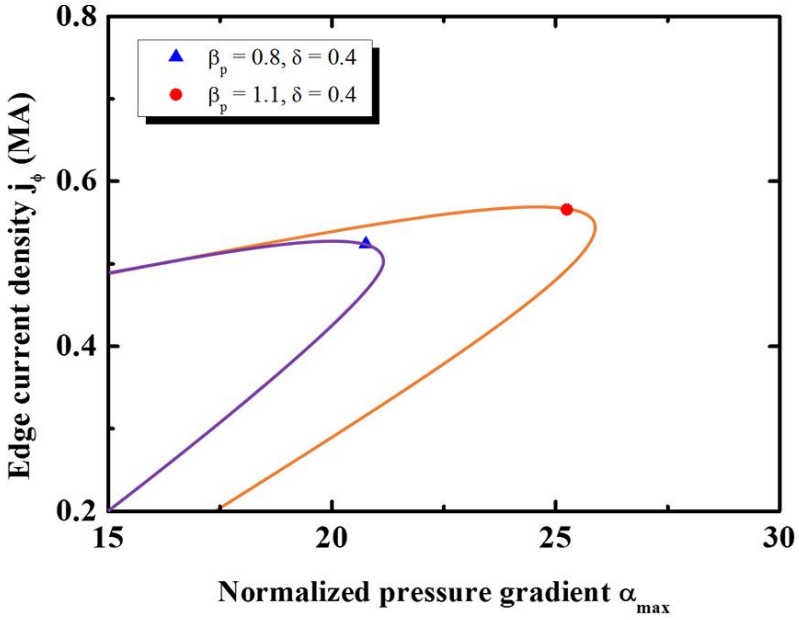


Fig. 5 Equilibrium point and stability boundary for different $\boldsymbol{\beta_p}$. Blue triangle corresponds to the critical equilibrium point for $\boldsymbol{\beta_p = 0.8}$, while red circle corresponds to that for $\boldsymbol{\beta_p = 1.1}$.

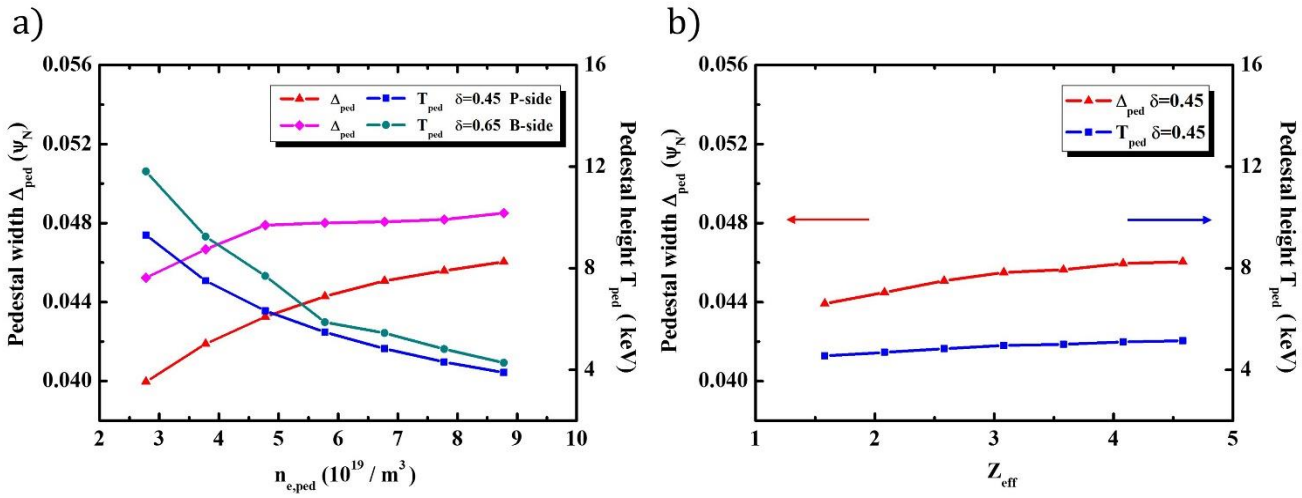


Fig. 6 $\Delta_{ped}$ and $T_{ped}$ as a function of (a) $n_{e,ped}$ and (b) $Z_{eff}$.

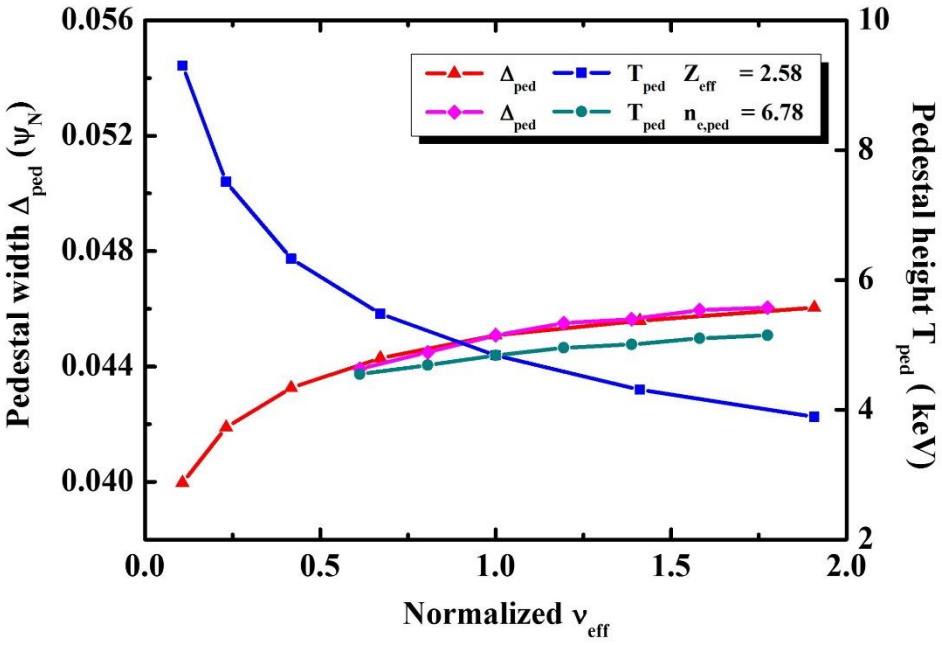


Fig. 7 $\boldsymbol{\Delta_{ped}}$ and $\boldsymbol{T_{ped}}$ as a function of $\boldsymbol{\nu_{eff}}$.

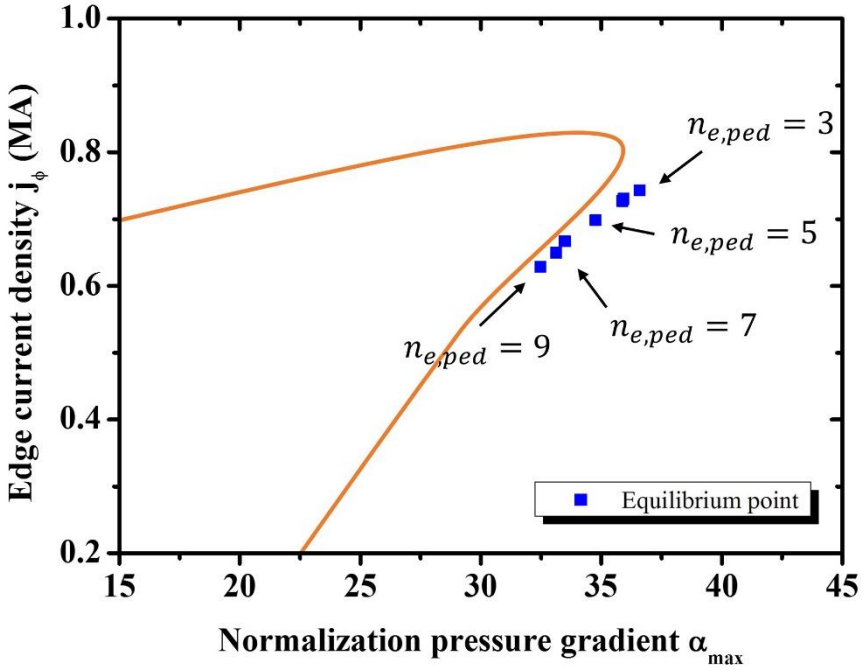


Fig. 8 Stability boundary and critical equilibrium points for different $\mathbf{n_{e,ped}}$ (in $\mathbf{10^{19}/m^3}$). Other plasma parameters except $\boldsymbol{\delta}$ ($\boldsymbol{\delta = 0.65}$) are same as those in reference plasma equilibrium.